

Effect of Cu and Co addition on CO gas-sensing properties of TiO₂ prepared by oxidation of mechanically-synthesized TiN composites

Youngki Cho^a, Yeontae Yu^b, Jaewon Lim^b and Jeshin Park^{b,*}

^aMetallurgical Engineering, Graduate School, Chonbuk National University, Jeonju 561-756, Korea

^bDivision of Advanced Materials Engineering and Research Centre for Advanced Materials Development, College of Engineering, Chonbuk National University, Jeonju 561-756, Korea

Cu- and Co-added TiO₂ sensing material composites were prepared by oxidizing TiN-Cu and TiN-Co composites that were synthesized using ball milling in an N₂ atmosphere. Structural characterization was performed using X-ray diffraction, field emission scattering electron microscopy (FE-SEM), and transmission electron microscopy (TEM). The pure, Co- and Cu-added TiO₂ sensing materials were prepared by oxidizing the synthesized TiN, TiN-Cu and TiN-Co powders at 600 °C. The additive Cu in the TiO₂ powder was changed to CuO crystals while the additive Co formed the CoTiO₃ phase. Therefore, the CuO phase was segregated and grown regardless of the TiO₂, however the additive Co in the TiO₂ was not cohered. The Co-added TiO₂ had greater responses than that of the Cu-added sample at all operating temperatures and showed the highest response of 5.32 at 1000 ppm CO gas. The higher sensing response of the Co-added TiO₂ resulted in an enhancement of the grain surface and incorporation with catalytic metals by highly dispersed Co.

Key words: Composites, Nanostructured materials, Mechanical milling, TiO₂ sensor material, Metal oxide semiconductor

Introduction

TiO₂ is nontoxic, chemically stable, and low-cost n-type sensing material compared to other common metal oxides such as SnO₂ and ZnO. TiO₂ powder has been examined for gas sensing and exhibited good sensing characteristics [1-4]. However, TiO₂ materials have drawbacks including low response, poor selectivity and stability [5]. The principle of operation of semiconductor gas sensors is based on the interaction of a gas molecule with the surface, which produces an interchange or trapping of free carriers. This sensing mechanism implies that the surface of the material is extremely important [6]. The high sensitivity for gases is supplied either by the surface of the grains or by a foreign material dispersed on them. Therefore, in order to obtain more sensitive surfaces, catalytic additives are incorporated into the base metal oxide [7-10]. The most typical manner for enhancing the sensing characteristics of TiO₂ has been the incorporation of catalytic noble metals, such as Au or Pd, or transition metals such as Co or Cu [11-15].

A mechanical alloying/milling technique can overcome fabrication difficulties, achieve high solid solubility, mix elements with a high vapor pressure and/or large differences in melting points, and produce amorphous and nanocrystalline materials [16-18]. Furthermore, it is

possible to produce solid–solid, solid-liquid, and solid-gas chemical reactions that cannot be realized at room temperature with this technique. A gas-solid reaction can dissociate or reform phases using the mechanical impact during a room-temperature mechanochemical process [19]. In the case of pure Ti, compounds can easily form with hydrogen, nitrogen, or oxygen because it is a highly reactive metal. Therefore, the mechanically induced gas-solid reaction is promising for the synthesis of materials with desired microstructures such as composite sensor materials [20-21].

In this work, mechanically-synthesized TiN was modified with different transition metals (Co, Cu), and TiN composites were oxidized to TiO₂ at several temperatures and characterized. The electrical measurements showed a particular behavior (n- or p-type) depending on the oxidation temperature. The main purpose was to investigate the effects of two transition metals (cobalt and copper) as additives on a TiO₂ sensing material.

Experimental procedure

Ti (purity 99.4%, -100 mesh), Cu (purity 99.85%, -100 mesh) and Co (purity 99.5%, -100 mesh) powders were used as the base material. Mechanical alloying was performed in a planetary high-energy ball mill under a pressurized N₂ atmosphere. The ball-to-powder weight ratio was 10 : 1. To prepare the powder for milling, approximately 20 g of the powder was placed in a stainless steel vial with stainless balls (10 mm in diameter). The disc and vial rotating speed were 600

*Corresponding author:
Tel : +82-63-270-2293
Fax: +82-63-270-2305
E-mail: parkjs@jbnu.ac.kr

and 320 rpm, respectively. The crystal structures of the synthesized and oxidized powders were analyzed via X-ray diffraction (XRD) using a Cu-K α source (Rigaku, D-Max 2500). The Brunauer-Emmett-Teller (BET) surface area was measured via nitrogen adsorption using a surface area analyzer (Micromeritics TRI-3000). The microstructures of the samples were observed using FE-SEM (Hitachi S-4800) and TEM (JEM-2010, JEOL).

To measure the sensor response of the pure, Cu- and Co-added TiO₂ powders, sensor devices were fabricated as follows: the unmodified, Cu- and Co-added TiO₂ powders were mixed with alpha-terpineol (C₁₀H₁₈O, 96%) and ground in an agate mortar for 30 min. The prepared pure, Cu- and Co-added TiO₂ pastes were applied to 15 × 15-mm alumina circuit boards, each with a 10 × 10-mm area of interdigitated Pt electrodes. These boards were then sintered at 600 and 800 °C in an electric furnace for 3 hrs. Resistance changes of these devices in response to the presence of the test gas were measured using a high-resistance meter (Agilent 34970A). These tests were performed at temperatures ranging from 200 to 550 °C and with various concentrations of CO (200-1000 ppm) in a temperature-controlled environment. The balance gas was N₂ and the air was mixed to 10.5% oxygen. The total gas flow rate was 100 mL/min. The sensor responses (R_s) of the n- and p-type sensors to CO gas were calculated using the equations of R_a/R_g and R_g/R_a , respectively, where R_a is the resistance in air with 10.5% O₂, and R_g is the resistance in the test and mixed gases.

Results and Discussion

Fig. 1 shows the XRD patterns of the pure, Cu- and Co-added Ti powders that were ball milled in a pressurized N₂ atmosphere for 25 hrs. The powders milled in the N₂ atmosphere consisted of a single phase of TiN. When the milled powders were oxidized in air at 600 °C, the TiN phases were changed to TiO₂, as shown in Fig. 2. The TiO₂ coexisted in the anatase and rutile phases. Concerning the effects of additives on TiO₂, it was qualitatively observed that additive Cu and Co promoted the anatase-to-rutile transformation. In contrast, diffractions that can be attributed to the additive metal oxides were not detected in the powders.

Fig. 3 shows the SEM images and particle distributions of the (a) pure, (b) Cu- and (c) Co-added TiO₂ powders that were oxidized at 600 °C. These powders were agglomerated by particles that were approximately 20-60, 20-90 and 20-70 nm in size, respectively. The mean sizes of the powders were 33.0, 55.3 and 42.0 nm, respectively. To confirm the existence of Cu and Co in the powders that were oxidized at 600 °C, element mappings were performed using EDS from the FE-SEM analysis. As shown in Fig. 4, three elemental mappings were observed in (a) Cu- and (b) Co-added powders, and these elements were uniformly distributed throughout the powders. It is worth noting that the well-distributed

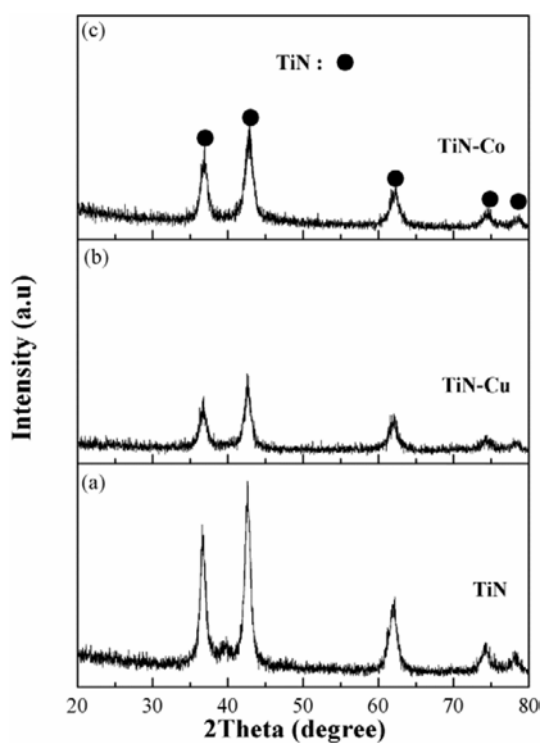


Fig. 1. XRD patterns of the milled powders under an N₂ atmosphere for 25 hrs.

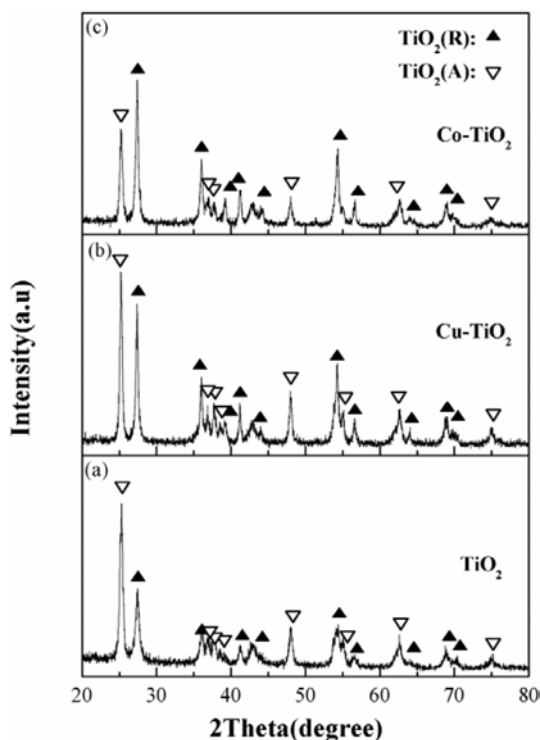


Fig. 2. XRD patterns of (a) TiO₂, (b) TiO₂-4Cu and (c) TiO₂-4Co powders oxidized at (a) 600 and (b) 800 °C.

Cu dots were more dense than those of Co, as shown in Fig. 4(a) and (b).

Microstructures of the (a) pure, (b) Cu- and (c) Co-added TiO₂ powders that were oxidized at 600 °C

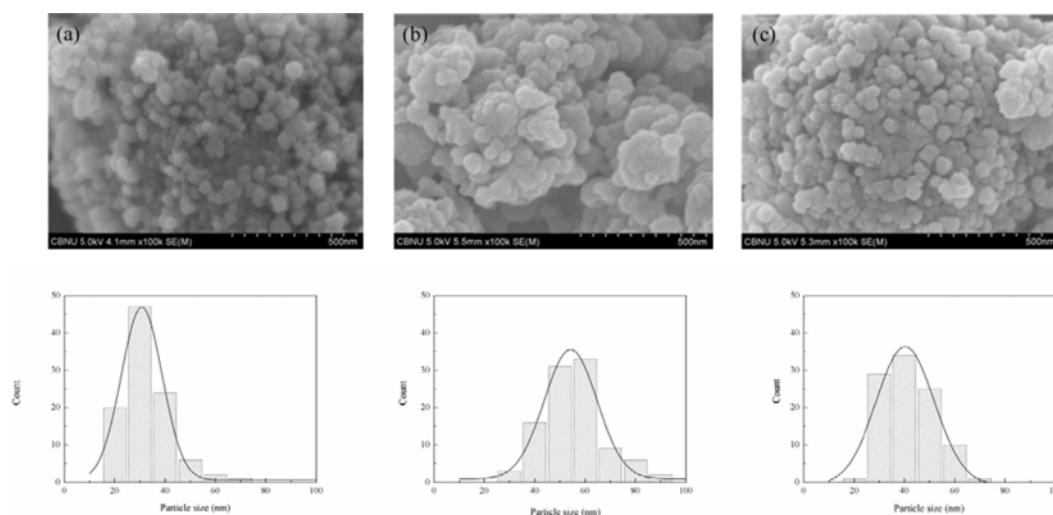


Fig. 3. FE-SEM images and particle distributions of (a) TiO₂, (b) TiO₂-4Cu and (c) TiO₂-4Co powders oxidized at 600 °C for 3 hrs.

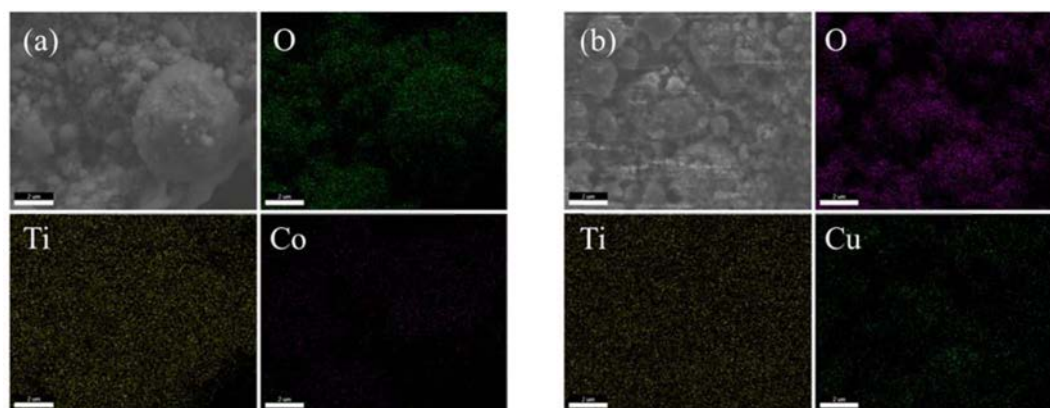


Fig. 4. FE-SEM images and EDS results of (a) TiO₂-4Co and (b) TiO₂-4Cu powders oxidized at 600 °C for 3 hrs.

Table 1. Crystallite sizes of anatase (D_a) and rutile (D_r), anatase content, and specific surface areas of samples oxidized at 600 and 800 °C.

Oxidation Temp.	600 °C					800 °C		
Samples	Anatase (%)	D_a (nm)	D_r (nm)	Particle size (nm)	SSA (m ² /g)	Anatase (%)	D_r (nm)	SSA (m ² /g)
TiO ₂	77.2	19.6	21.7	33.0	10.24	5.0	56.3	3.50
Cu-TiO ₂	64.2	29.9	30.0	55.3	4.24	–	42.3	2.08
Co-TiO ₂	48.7	26.1	25.7	42.0	6.02	–	34.1	2.32

were investigated using TEM, including light field image diffraction-mode images, and dark field images corresponding to the TiO₂ planes. As shown in Fig. 5, the TiO₂ size in (a) pure, (b) Cu- and (c) Co-added powders ranged from 15 to 40 nm, 15 to 46 nm and 13 to 38 nm, respectively.

When the oxidation temperature of the powders was increased to 800 °C, mixed phases of anatase and rutile changed to the rutile phase and distinct CuO peaks appeared in the (b) Cu-added powder. However, the CoTiO₃ phase was precipitated in the (c) Co-added powder, as shown in Fig. 6.

Fig. 7 shows three elemental mappings of (a) Cu-

and (b) Co-added powders that were performed using EDS from the FE-SEM analysis. The Cu dots in Fig. 7(a) cohered, while the Co dots in Fig. 7(b) were uniformly distributed. The method for the equilibrium state was different between Cu and Co additives in TiO₂, i.e. the Cu additive was changed to CuO crystals while the additive Co in the TiO₂ powder formed the CoTiO₃ phase (see Fig. 6). Therefore, the CuO phase could be segregated and grown regardless of the TiO₂, however the Co dot in Fig. 7(b) should not be cohered because the CoTiO₃ phase was formed by reaction between the Co additive and TiO₂ of the matrix.

Table 1 summarized the anatase content, crystallite

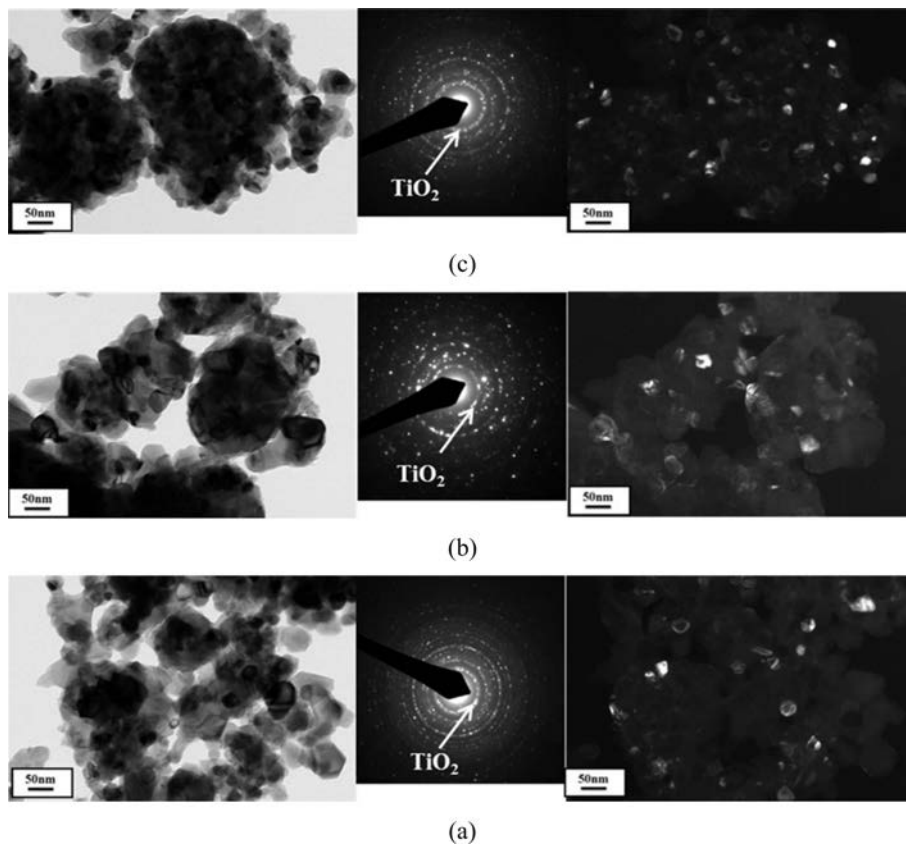


Fig. 5. TEM images of (a) TiO_2 , (b) $\text{TiO}_2\text{-4Cu}$ and (c) $\text{TiO}_2\text{-4Co}$ powders oxidized at $600\text{ }^\circ\text{C}$ for 3 hrs.

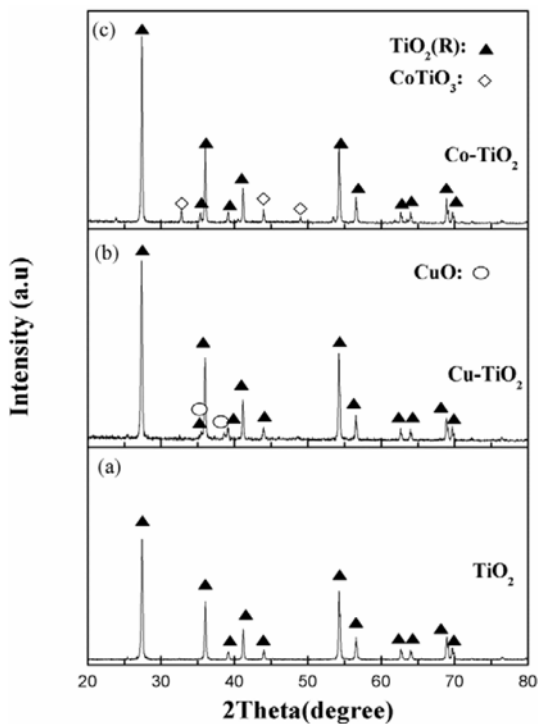


Fig. 6. XRD patterns of (a) TiO_2 , (b) $\text{TiO}_2\text{-4Cu}$ and (c) $\text{TiO}_2\text{-4Co}$ powders oxidized at $800\text{ }^\circ\text{C}$.

size, particle size and specific surface area (SSA) of the pure, Cu- and Co-added TiO_2 powders that were

oxidized at 600 or $800\text{ }^\circ\text{C}$. The crystallite sizes of anatase (D_a) and rutile (D_r) were determined from the diffraction peak broadening using the Debye-Scherrer equation, and the anatase percentages were determined using the intensities of the anatase (1 0 1) and rutile (1 1 0) reflections [22]. At $600\text{ }^\circ\text{C}$, all of the samples exhibited the anatase phase and the content in order of the pure, Cu- and Co-added TiO_2 powders. The grain size and particle size of the pure TiO_2 were the smallest while those of the Co-added powder were smaller than the Cu-added sample. The SSA decreased in order of the pure, Co- and Cu-added powders. The powders that formed at $800\text{ }^\circ\text{C}$ were primarily in the rutile phase with larger grain sizes.

To evaluate the gas sensing properties of the TiO_2 samples, the electrical resistances were measured at various CO concentrations for the TiO_2 samples with unmodified, Cu, and Co that were oxidized at (a) 600 and (b) $800\text{ }^\circ\text{C}$, as shown in Fig. 8. An experiment was conducted to test the n-type response to CO gas of the devices that were fabricated from TiO_2 powders with unmodified, Cu, and Co oxidized at $600\text{ }^\circ\text{C}$. However, the powders that were oxidized at $800\text{ }^\circ\text{C}$ exhibited p-type behavior, where the resistance of the sample increased after the exposure to CO. The change to the p-type by oxidizing at $800\text{ }^\circ\text{C}$ is believed to be related to precipitation of CuO or CoTiO_3 , as shown in Fig. 6. This precipitation could result in a conduction pathway through CuO or CoTiO_3 , which is a p-type semiconductor.

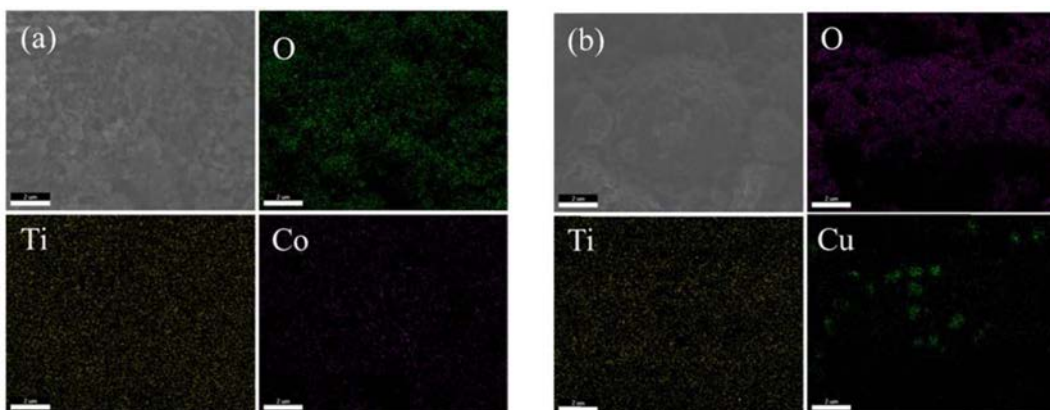


Fig. 7. FE-SEM images and EDS results of (a) TiO₂-4Co and (b) TiO₂-4Cu powders oxidized at 800 °C for 3 hrs.

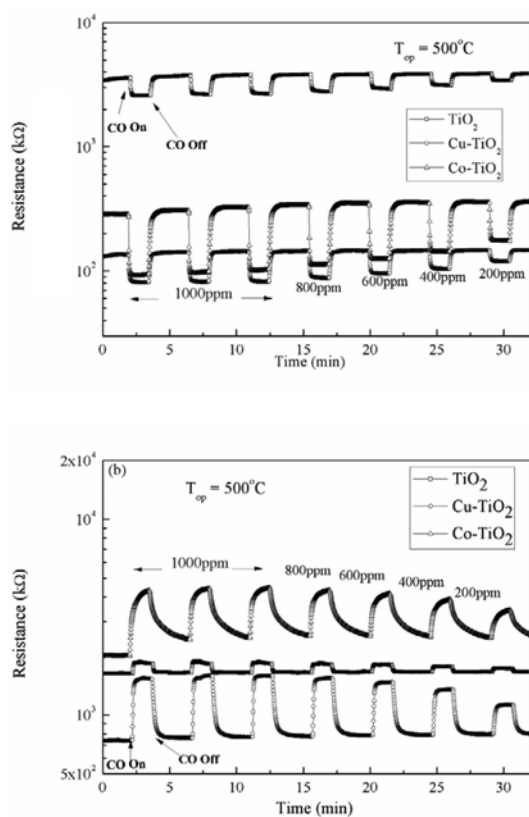


Fig. 8. Comparison of CO sensitivities at 400 °C of TiO₂-4Co and TiO₂-4Cu powders oxidized at (a) 600 and (b) 800 °C.

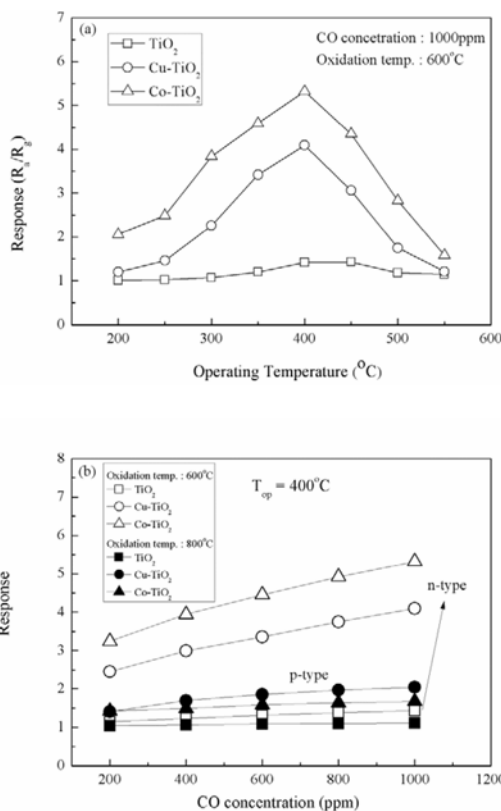


Fig. 9. Response of TiO₂-Cu powders oxidized at 600 °C to (a) 1000 ppm CO gas vs. temperature and (b) responses vs. CO concentration.

Fig. 9 shows the sensor responses to (a) an operating temperature of 400 °C and (b) CO gas concentrations for TiO₂ with unmodified, Cu and Co oxidized at 600 °C. The CO gas-sensing performance of n-type TiO₂ was enhanced by the addition of Cu and Co at all operating temperatures. It is well known that dispersed Cu or Co in TiO₂ acts as a catalyst for the oxidation of CO gas [23]. The responses of the devices increased up to 400 °C and then decreased when over 450 °C, as shown in Fig. 9(a). The device with Co had the highest responses at all operating temperatures and showed the highest response of 5.32 at 1000 ppm CO gas, whereas the CO response value of the pure and Cu-added TiO₂

were 1.2 and 4.9 under identical conditions, respectively. Regarding the sensor response as a function of the concentration of CO, the responses of TiO₂ with Cu and Co increased with increasing CO concentration and that of TiO₂ with Co was greater than that of the sample with Co at all CO concentrations, while that of pure TiO₂ was nearly constant at all concentrations of CO.

Previous research prepared TiO₂ as a gas sensing material via a wet chemical process [24-25]. Two important points should be noted regarding this work. One point is the difference in the preparation processes of TiO₂ powders modified with Cu and Co. The wet process requires multiple steps, increased handling requirements

and generation of waste during intermediate synthesis steps [20-21]. However, it is important that the mechanochemical method employed in this study was able to perform the preparation process in only two steps with the synthesis of TiN with Cu or Co and oxidization to Ti-Cu or Ti-Co oxide composites to overcome the faults of the wet processes. The second notable observation relates to the differences in sensing performance between the TiO₂ powders with Cu and Co. The precipitated phase in the sample with Cu oxidized at 800 °C was CuO, while that of the sample with Co was CoTiO₃. The CuO phases were segregated and grew regardless with TiO₂, while CoTiO₃ phases were uniformly distributed at high temperature, as shown in Figs. 6 and 7. CoTiO₃ phases were theorized to precipitate in the grain boundaries, therefore they would inhibit the growth of the TiO₂ phase. Therefore, the higher sensing response of Co-added TiO₂ results in an enhanced catalytic reaction and an enlarged reaction area by highly-dispersed Co, which acts as a catalyst for the oxidation of CO gas and an inhibitor of growth of the TiO₂ phase by oxidizing to CoTiO₃.

Conclusions

Cu- and Co-added TiO₂ sensing material composites were prepared by the oxidizing TiN-Cu and TiN-Co composites that were synthesized using ball milling in an N₂ atmosphere. The addition of Cu and Co to TiO₂ promoted an anatase-to-rutile transformation and grain growth. The responses of TiO₂ powders that were oxidized at 600 °C to CO gas were enhanced by the addition of Cu and Co. The enhancement is believed to originate from well-dispersed Cu and Co oxides, which are known catalysts for the oxidation of CO gas. Co-added TiO₂ showed the highest response of 5.32 at 1000 ppm CO gas. The superior sensing responses of the Co-added TiO₂ powder resulted in the enhancement of the grain surface and incorporation with catalytic metals by highly dispersed Co on the surface.

Acknowledgments

This research was supported by the Basic Science Research Program through the National Research Foundation of Korea (NRF) funded by the Ministry of Education (2014R1A1A2057485).

References

1. L. Sun, L. Huo, H. Zhao, S. Gao, J. Zhao, *Sens. Actuat. B* 114 (2006) 387-391.
2. A. Teleki, N. Bjelobrk, S.E. Pratsinis, *Sens. Actuat. B* 130 (2008) 449-457.
3. A. Teleki, S.E. Pratsinis, K. Kalyanasundaram, P.I. Gouma, *Sens. Actuat. B* 19 (2006) 683-690.
4. M. Yang, L.H. Huo, H. Zhao, S. Gao, Z. Rong, *Sens. Actuat. B* 143 (2009) 111-118.
5. X. Cheng, Y. Xu, S. Gao, H. Zhao, L. Huo, *Sens. Actuat. B* 155 (2011) 716-721.
6. A. Ruiz, A. Cornet, K. Shimano, J.R. Morante, N. Yamazoe, *Sens. Actuators B* 108 (2005) 34-40.
7. A. Cabot, J. Arbiol, J.R. Morante, U. Weimar, N. Barsan, W. Gopel, *Sens. Actuators B* 70 (2000) 87-100.
8. A.M. Ruiz, A. Cornet, K. Shimano, J.R. Morante, N. Yamazoe, *Sens. Actuators B* 108 (2005) 34-40.
9. N. Yamazoe, Y. Kurokawa, T. Seiyama, *Sens. Actuators B* 4 (1983) 283-289.
10. S.H. Hahn, N. Barsan, U. Weimar, *Sens. Actuators B* 78 (2001) 64-68.
11. N. Yamazoe, Y. Kurokawa, T. Seiyama, *Sens. Actuat. B* 4 (1983) 283-289.
12. H. Yamaura, J. Tamaki, K. Moriya, N. Miura, N. Yamazoe, *J. Electrochem. Soc.* 144 (1997) 158-160.
13. N. Yamazoe, *Sens. Actuat. B* 5 (1991) 7-19.
14. N. Yamazoe, N. Miura, J. Tamaki, *Trans. Mater. Res. Soc. Jpn.* A15 (1994) 111-116.
15. S. Matsushima, T. Maekawa, J. Tamaki, N. Miura, N. Yamazoe, *Chem. Lett.* (1989) 845-848.
16. S. Ozcan, M. M. Can, A. Ceylan, *Mater. Lett.* 64 (2010) 2447-2449.
17. B. Avar, M. Gogebakan, *J. Optoelectron. Adv. Mater.* 11 (2009) 1460-1463.
18. T.P. Yadav, R.M. Yadav, D.P. Singh, *Nanosci. Nanotechnol.* 2 (2012) 22-48.
19. Y.K. Cho, Y.T. Yu, S.Y. Yang, J.S. Park, *Ceram. Int.* 41 (2015) 13589-13597.
20. J.S. Park, C.H. Lim, Y.K. Cho, Y.T. Yu, *Met. Mater. Int.* 21 (2015) 330-336.
21. C.H. Lim, H.S. Kim, Y.T. Yu, J.S. Park, *Met. Mater. Int.* 20 (2014) 323-328.
22. A.M. Ruiz, G. Dezaneeu, J. Arbiol, A. Cornet, J.R. Morante, *Chem. Mater.* 16 (2004) 862-871.
23. N.O. Savage, S.A. Akbar, P.K. Dutta, *Sens. Actuat. B* 72 (2001) 239-248.
24. A.M. Ruiz, A. Cornet, K. Shimano, J.R. Morante, N. Yamazoe, *Sens. Actuat. B* 108 (2005) 34-40.
25. A.M. Ruiz, A. Cornet, K. Shimano, J.R. Morante, N. Yamazoe, *Sens. Actuat. B* 109 (2005) 7-12.